In Situ Fibrous Structure Oriented Polymer Blends Composed of Poly(lactic acid) and Polycaprolactone Containing Peroxide

Takeshi Semba,[1] Kazuo Kitagawa,[1] Masaya Kotaki,[2] Hiroyuki Hamada[2]

[1]*Organic Materials Laboratory, Kyoto Municipal Industrial Research Institute, Industrial Research Center, 134 Chudoji Minami-machi, Shimogyo-ku, Kyoto 600-8813, Japan*
[2]*Division of Advanced Fibro-Science, Kyoto Institute of Technology, Gosyokaido-cho, Matsugasaki, Sakyo-ku, Kyoto 606-8585, Japan*

Received 20 July 2007; accepted 5 October 2007
DOI 10.1002/app.27587
Published online 27 December 2007 in Wiley InterScience (www.interscience.wiley.com).

ABSTRACT: A fibrous dispersed phase stuffed with polycaprolactone (PCL) was constructed in a poly(lactic acid) (PLA) matrix during an injection-molding process. The injection-molding process showed efficiency in forming dispersions with fibrous shapes, and they could impart the ductile property of PCL to the brittle PLA matrix, with appropriate interfacial adhesion arising from the cocrosslinking structure at the PLA/PCL interface by dicumyl peroxide (DCP). However, the addition of excess DCP caused a split of the dispersions resulting from the compatibility increment and the excess crosslinking reaction at the interface and inside each phase. The addition of a small amount of DCP could adhere the interface without splitting of the dispersions. The observed internal structure in the injection moldings showed a morphology transition that changed gradually from a fine fibrous morphology to a coarse morphology at a deeper position in the injection moldings. The tensile properties of sliced local layers, which were fabricated with a sliding microtome, proved that the fibrous morphology was effective in the improvement of ductility of the blends. An X-ray analysis showed that the shear flow increased the crystalline orientation and formed a different crystalline structure only in the PCL dispersed phase, but its crystalline structure was not the main factor for ductility improvement. © 2007 Wiley Periodicals, Inc. J Appl Polym Sci 108: 256–263, 2008

Key words: blends; morphology; shear

INTRODUCTION

The use of poly(lactic acid) (PLA) as a biobased polymer has been expanding in various applications such as automobiles and portable instruments (e.g., cell phone and music players).[1–3] These achievements are due to advanced composites technology, which is a combination of PLA, a microfiller or nanofiller, natural fibers, and so on, to gain high heat resistance, high rigidity, and strength. However, PLA composites need to overcome another drawback, the brittleness of PLA, to attain further expansion of its use. Some attempts to improve fracture toughness were carried out with the application of various impact modifiers such as synthetic elastomers[4] or other petroleum polymer materials,[5,6] natural rubbers,[7] and other biodegradable polymers.[8–10] The most effective modifiers were synthetic elastomers or petroleum polymer materials. In the former case, some chemical modification on the molecular end was applied for an increase in the compatibility with the PLA matrix, which had an effect on the impact properties. In the latter case, various other recycled petroleum polymers—poly(methyl methacrylate), polycarbonate and poly(ethylene terephthalate)—were added to PLA. These investigations were aimed at the development of ecomaterials using recycled petroleum polymers, and the original compatible technologies were applied to these blends. Recently, ecomaterials such as PLA/natural rubber blends were introduced. They showed that the high impact strength and high biobased content were consistent with keeping the biodegradability. The study of PLA and other biodegradable polymer blends has also been actively studied. In these studies, ductile biodegradable polymers such as poly(butylene succinate) and polycaprolactone (PCL) were used for improving the impact strength.

We also have been trying to improve the brittleness to yield high-performance materials to use in various applications.[11–13] Dicumyl peroxide (DCP) was used as a cocrosslinked agent that could enhance the interfacial adhesion between the PLA matrix and dispersed PCL. The ultimate tensile strain and impact strength of the blends containing DCP were far superior to those of the blends without DCP. Furthermore, it was clear that the compounding procedure, by means of a side feeder, affected

Correspondence to: T. Semba (sentake@city.kyoto.jp).

Journal of Applied Polymer Science, Vol. 108, 256–263 (2008)

the mechanical properties and disperse phase morphology; in other words, the addition of DCP at the middle of the extruder was more effective.[14] This DCP addition at the side feeder brought some decisive effects, such as firm interfacial adhesion, fine dispersions, and ductility increment of the dispersed PCL phase.

On the other hand, we have been trying to develop an *in situ* fiber reinforced polymer blend in which the dispersed phase is formed into a fibrous morphology during polymer processing.[15–17] The dispersed fibers could improve the modulus and strength while maintaining ductility. However, these investigations have not taken into consideration ecomaterials; therefore, biodegradation and biobased content were taken up in this study. This study was aimed at the settlement of PLA brittleness by the use of the aforementioned two techniques: the interfacial cocrosslinking method and *in situ* fiber reinforcing technique. To be concrete, the PLA/PCL blends containing DCP were molded into injection moldings to construct the fiber reinforcements by shear flow. Consequently, to yield a highly biobased, high-ductility, and biodegradable material that can be used for practical purposes is the ultimate goal of this sequence of studies.

EXPERIMENTAL

Materials and compounding

The materials used in this study were PLA (melt index = 8.0 g/10 min, weight-average molecular weight = 150,000; Lacea H100, Mitsui Chemicals, Inc., Tokyo, Japan), PCL (melt index = 2.3 g/10 min, weight-average molecular weight = 160,000; Cel Green PH7, Daicel Chemical Industries, Ltd., Osaka, Japan), and DCP (half-life at 175°C = 1 min; NOF Corp., Tokyo, Japan).

The materials were blended with a twin-screw extruder (screw diameter (φ) = 15, length/diameter = 60; Technovel Corp., Osaka, Japan). The blend ratio of PLA to PCL was 70/30 by weight. The investigated DCP contents were 0, 0.1, 0.2, and 0.3 phr, which were determined as the optimum concentrations in our previous investigations.[11] The screw configuration consisted of four kneading and other full-flight zones. Compounding was performed at a cylinder temperature of 180°C and a screw revolution of 80 rpm.

Injection molding

The compounded materials were molded into dumbbell-shaped injection moldings with 1-mm thickness by means of an injection molding machine (maximum cavity pressure = 30 ton; Ti30F6, Toyo Machinery & Metal Co., Ltd., Hyogo, Japan). The cylinder and mold temperatures were 180 and 25°C, respectively. The injection speed and holding pressure were 20.8 cm^3/s and 120 MPa.

To investigate the injection speed dependence on the mechanical properties, samples with various injection speeds were molded. The injection speeds of 3.2, 9.6, 20.8, and 28.8 cm^3/s were applied to the blend containing 0.1 phr DCP.

Evaluations of the mechanical properties and fracture aspects of the injection moldings

Standard tensile tests with dumbbell-shaped specimens were carried out with a universal testing machine (Autograph AG-5000E, Shimadzu Corp., Kyoto, Japan) at a tensile speed of 50 mm/min while the specimen gauge length was 25 mm. The testing temperature was 23°C. The fracture surface was observed with a scanning electron microscope (JSM5900LV, JEOL, Ltd., Tokyo, Japan).

Observation of the microstructure in injection moldings

The cross sections of injection moldings were observed with atomic force microscopy (AFM; Nanoscope IIIa, Digital Instruments Co., Ltd., California), which is capable of distinguishing each component of PLA/PCL blends. The observed area was planed with a microtome (HM360, Microm International GmbH, Walldorf, Germany) equipped with a glass knife. The tapping mode, which is a commonly used observation method in AFM, was applied to the cross-sectional area, and the phase images were captured.

Fabrication of sliced samples of injection moldings

An interesting study on the internal morphology around the weld line formed in injection moldings was reported by means of an evaluation of sliced specimens.[18] The same method was taken up to verify the relationship between the mechanical properties and microstructure of injection moldings. The injection moldings with 0.1 phr DCP, molded at an injection speed of 20.8 cm^3/s and holding pressure of 120 MPa, were sliced with a sliding-type microtome (SM2500S, Leica Microsystems GmbH, Wetzlar, Germany). The slicing speed was set as slow as 1.5 mm/s to prevent the relaxation of molecular orientation, and the thickness of the sliced specimens was 50 μm for tensile testing. Furthermore, the sliced specimens with a thickness of 100 μm were prepared by the same procedure, and the sliced samples were used to investigate the crystalline structure with wide-angle X-ray diffraction (WAXD).

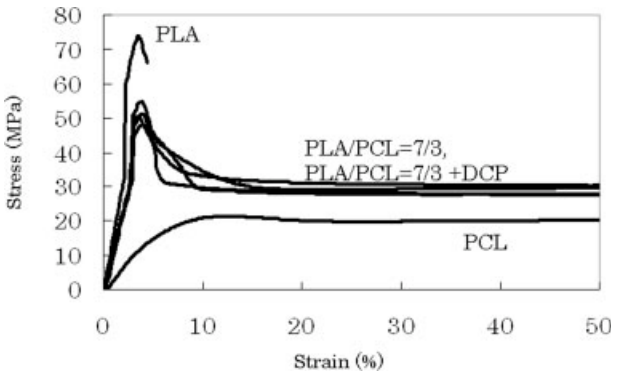

Figure 1 Stress–strain curves of injection moldings.

Characterization of internal local layers of injection moldings

Tensile tests of sliced specimens with a 50-μm thickness were carried out under the same conditions as those used for the dumbbell-shaped injection moldings. Furthermore, WAXD patterns were obtained with an X-ray diffraction machine [R-AXIS IV, Mo Kα (λ = 0.71 Å), Rigaku Corp., Tokyo, Japan].

RESULTS AND DISCUSSION

Mechanical properties and fracture aspects

The stress–strain curves of injection moldings molded at an injection speed of 20.8 cm^3/s are shown in Figure 1. PLA showed the highest modulus and maximum stress but the lowest strain at break. On the other hand, PCL showed a low initial slope indicating low modulus and low maximum stress but a very large ultimate strain. All the blend specimens showed an ultimate tensile strain greater than 50% with accompanying yield stress and necking phenomena. The tensile properties as a function of the DCP content are elaborated in Figure 2. The tensile modulus and strength of the blend specimens exhibited almost constant values throughout the entire DCP dosage. However, the ultimate tensile strains of the blend specimens were different, depending on the DCP dosage. The ultimate tensile strain of the blend without DCP showed the smallest value of 50%, and the maximum strain at break was obtained at 0.1 phr DCP. The peak value was reached at 300%. In this study, the large ultimate tensile strain of the blend with 0.1 phr DCP was the main consideration.

Scanning electron micrographs of the fracture surface are shown in Figure 3. The blend without DCP showed a flat fracture surface that described the occurrence of brittle fracture [Fig. 3(a)]. On the other hand, a section in which the fibrous fracture could be seen at a high magnification was observed on the fracture surface of the blend containing 0.1 phr DCP [Fig. 3(b)]. This described the occurrence of ductile fracture. The ductile fracture section vanished with increasing DCP content, and the fracture aspect showed brittleness. That is, the ductile fracture section of the blend containing 0.3 phr DCP could not be observed [Fig. 3(c)]. It was concluded that the addition of DCP had some effects on the dispersed morphological development of the dispersed phase and interfacial adhesion.

Microstructure of injection moldings

The microstructure of injection moldings with various DCP contents was observed to verify how it affected the ultimate tensile strain and its fracture behavior. The AFM images of the internal structure and schematic drawings are shown in Figure 4. Three parts in the thickness direction of the injection moldings—the skin, intermediate, and core—were

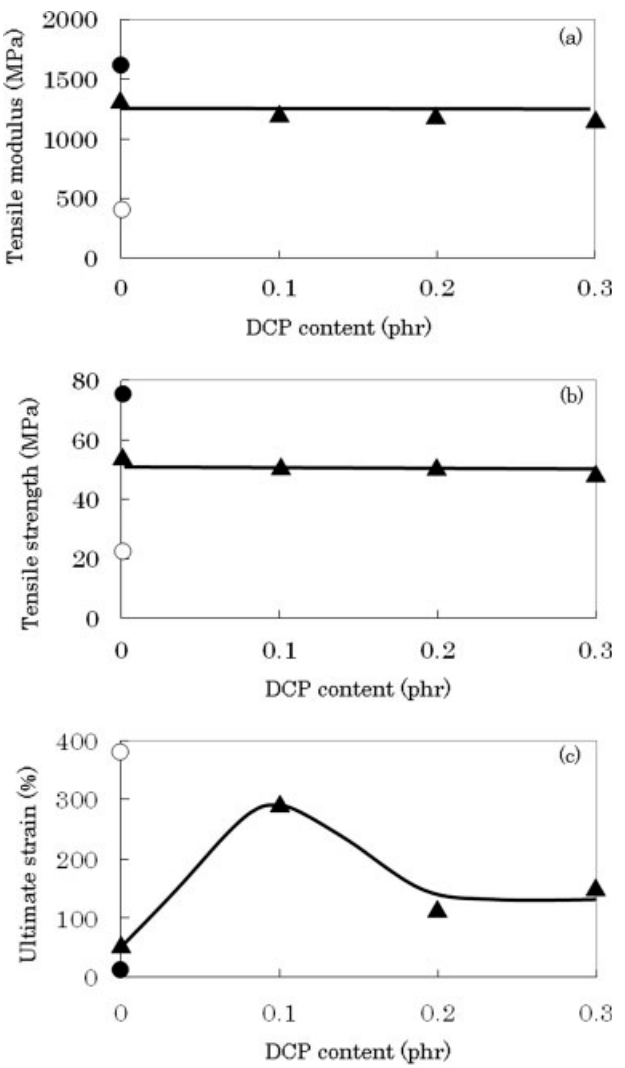

Figure 2 (a) Tensile modulus, (b) tensile strength, and (c) ultimate strain of injection moldings: (●) neat PLA, (▲) 70/30 PLA/PCL, and (○) neat PCL.

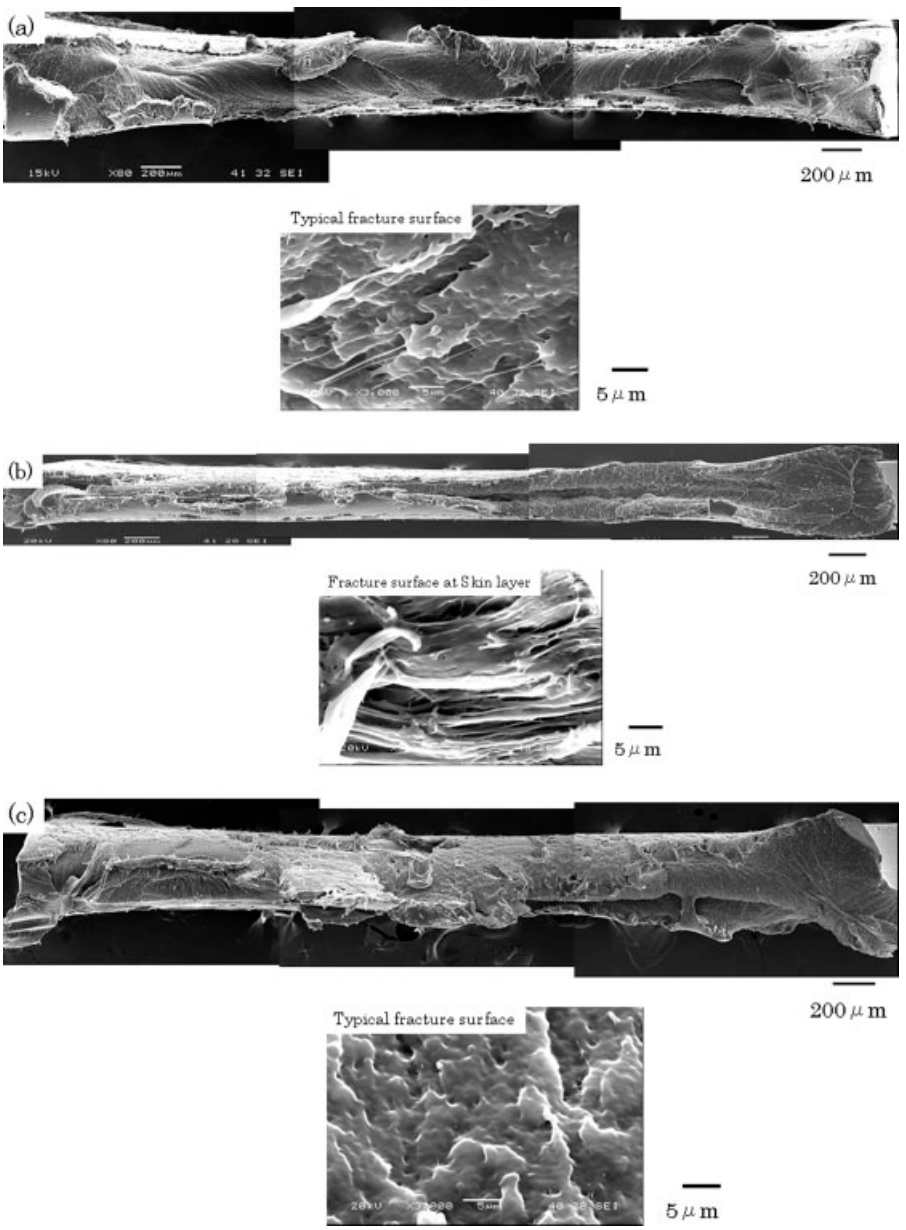

Figure 3 Fracture surface of blend specimens: (a) 70/30 PLA/PCL, (b) 70/30 PLA/PCL + 0.1 phr DCP, and (c) 70/30 PLA/PCL + 0.3 phr DCP.

observed. In the case of the blend without DCP [Fig. 4(a)], the marble morphology was formed at the skin part along the flow and transverse directions; that is, the morphology at the skin part could be regarded as a thin, flat, fibrous shape with a thickness of about 100 nm. Thus, the *in situ* fiber formation could be observed in the injection moldings consisting of PLA and PCL. The morphology was steadily changed and became coarser at deeper positions in which the thicknesses were a few hundred nanometers at the intermediate part, and its shape approached an ordinary fibrous shape. The thickness at the core part became almost 1 μm. The length of the fibrous dispersed phase at the skin and intermediate parts could not be measured because the fibrous structure lay along the whole length of the image frame of 5 μm. On the other hand, the length at the core part appeared to be shorter than that at skin and intermediate parts. The shear flow during the injection process could transform the dispersions of the blend without DCP into fibers because it includes flexible dispersions without crosslinking.

Figure 4(b) shows the AFM images and schematic drawings of the blend containing 0.1 phr DCP. The thicknesses of the flat fiber at the skin part and the ordinary fiber at the intermediate part were coarser than that of the blend without DCP, but they maintained thicknesses less than 1 μm and barely kept a

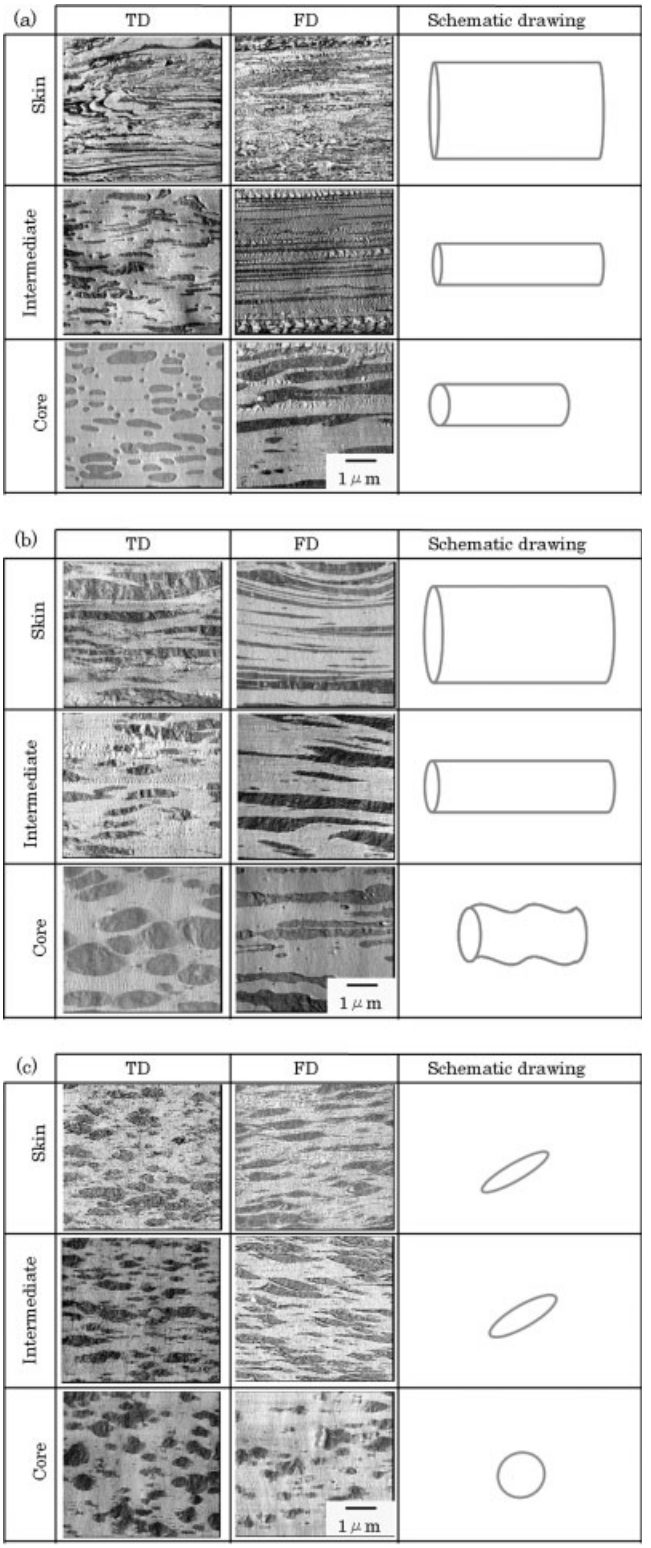

Figure 4 AFM image and schematic drawing of the internal structure: (a) 70/30 PLA/PCL, (b) 70/30 PLA/PCL + 0.1 phr DCP, and (c) 70/30 PLA/PCL + 0.3 phr DCP.

fibrous structure with a smooth contour; this means that the dispersions were deformed by sufficient shear flow. Finally, the continuous phase appeared to have a distorted contour at the core part along the flow direction; that is, the continuous phase was about to be split because of stress relaxation and insufficient shear flow. Further strong shear flow would be needed to construct a smooth contour for the dispersed phase.

Drastic changes in contrast to the blend without and with 0.1 phr DCP could be seen in the blends containing 0.2 or 0.3 phr DCP. Figure 4(c) presents AFM images and schematic drawings of the blend containing 0.3 phr DCP. The split dispersions were distributed throughout from the skin to core part. At the skin and intermediate parts, the thickness of dispersions was about 500 nm, and the length was only 1–3 μm. The length at the core part was 0.5–1 μm with the same thickness of skin and intermediate parts. Thus, the extinction of fibrous morphology was especially notable in the blend containing 0.2 or 0.3 phr DCP. The continuous dispersions were split into pieces throughout whole layers during the injection-molding process. It was inferred that this phenomenon was enhanced by the loss of the mobility and flexibility of dispersions due to crosslinking and cocrosslinking.[11]

Thus, in the case of the blend containing 0.2 or 0.3 phr DCP, the fibrous morphology almost vanished. The ultimate tensile strain of these samples was larger than that of the blend without DCP by the improvement of interfacial adhesion attributed to cocrosslinking.[11–13] It was noteworthy that the 300% ultimate tensile strain of the blends with 0.1 phr DCP was prominent for all the specimens. The flat and ordinary fibrous morphology, covered from the skin to the intermediate layer in the injection moldings, would enhance the ultimate tensile strain more than the coarser and split dispersions as distributed in the blends with 0.2 or 0.3 phr DCP. Furthermore, the interface was bonded because of 0.1 phr DCP; that is, the blend with 0.1 phr DCP had these two advantages, a fibrous morphology and interfacial adhesion. The fibrous morphology with the interfacial adhesion formed a ductile fracture surface. On the other hand, the fracture surface of the blend

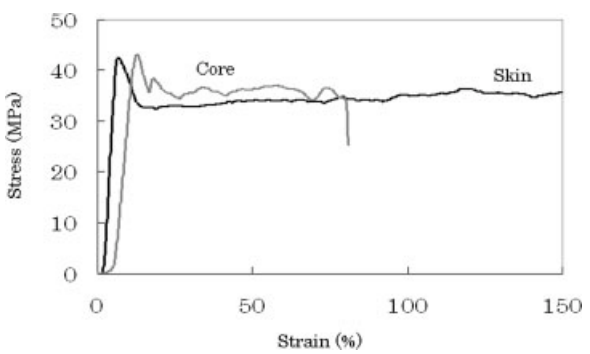

Figure 5 Stress–strain curves of 70/30 PLA/PCL + 0.1 phr DCP in the skin and core local layers.

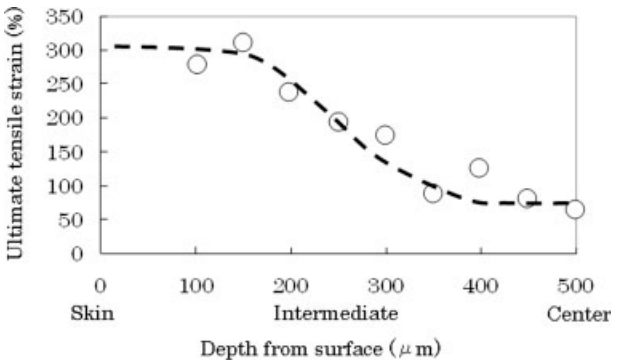

Figure 6 Ultimate tensile strain of a sliced sample fabricated from the blend with 0.1 phr DCP.

with 0.2 or 0.3 phr DCP exhibited a flat aspect due to split dispersions.

Ultimate tensile strain of local layers

Tensile testing of sliced specimens prepared from the injection-molded specimens was conducted to understand the mechanisms of the high ultimate tensile strain of the blend with 0.1 phr DCP. Figure 5 shows typical tensile stress–strain curves of skin and core local layers of the blend with 0.1 phr DCP. The sliced specimens in the skin part displayed higher ultimate tensile strain over 150%; on the other hand, those in the core part displayed a strain of about 80%. This extreme difference of ultimate tensile strain between skin and core parts must affect the tensile ductility of the injection moldings.

Figure 6 shows the ultimate tensile strain of local layers as a function of depth from the surface. The ultimate tensile strain implied the existence of a morphology transition in injection moldings with 0.1 phr DCP for their value remained constant from the surface to a depth of 150-μm, then suddenly decreased up to 390 μm, and finally stayed low and constant toward the core of the injection moldings. These three distinct layers were named the initial plateau, reduction, and second plateau areas in this study. The behavior of the ultimate tensile strain of local layers was compared with the morphology observation results of AFM. It was revealed that the flat, fibrous morphology of the finely dispersed PCL phase stimulated the high ultimate tensile strain in the initial plateau area. The ordinary fibrous morphology in the reduction area could keep a higher ultimate tensile strain in contrast to the distorted, coarse PCL dispersions in the second plateau area. From these results, the initial plateau area consisted of the flat, fibrous morphology, especially showing efficiency at achieving high ultimate tensile strain. Therefore, the ultimate tensile strain of the blend with 0.1 phr DCP was the best of all because of the two benefits, which were the fibrous morphology by the construction of strong shear flow and interfacial adhesion by DCP.

Crystalline orientation and structure of local layers in injection moldings

Shear flow often induces crystalline orientation, crystallization, alternations of crystalline structure, and so forth.[19,20] In a previous study, we found a crystallinity increment of PCL dispersions with a fibrous shape in the polyolefin matrix.[16] There may be a possibility of such changes in the dispersed PCL phase in the PLA matrix. Here, WAXD patterns were taken to gain information about the crystalline structure and orientation. Figure 7 presents the WAXD patterns of local layers at the depths of 100, 300, and 500 μm from the surface of injection moldings containing 0.1 phr DCP. The deep spots derived from the PCL phase appeared on the equator at depths of 100 and 300 μm from the surface. At a depth of 500 μm from the surface, the spots on the equator became weaker than the points at 100 and 300 μm. Figure 8 shows the X-ray diffraction intensity along the equator of each sample calculated from Figure 7. The strong and weak 2θ diffraction peaks derived from the PCL phase occurred at 9.5, 9.7, and 10.7°, and all of them indicated a decrement at deeper points. The shoulder peak at 9.5°, able to be observed at a depth of 100 μm from the surface,

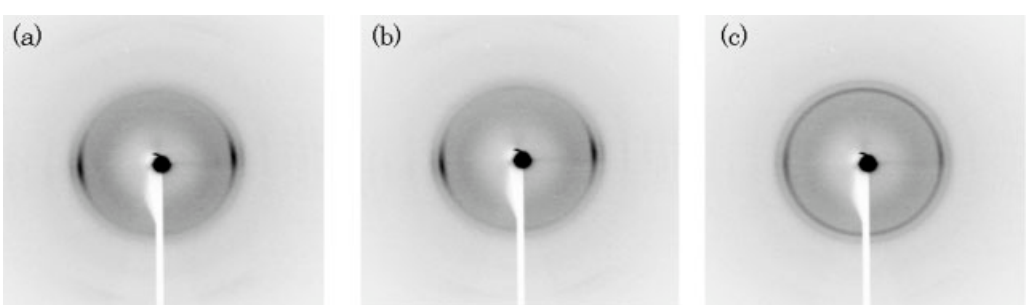

Figure 7 X-ray diffraction patterns of 70/30 PLA/PCL + 0.1 phr DCP at each layer: (a) depth of 100 μm, (b) depth of 300 μm, and (c) depth of 500 μm.

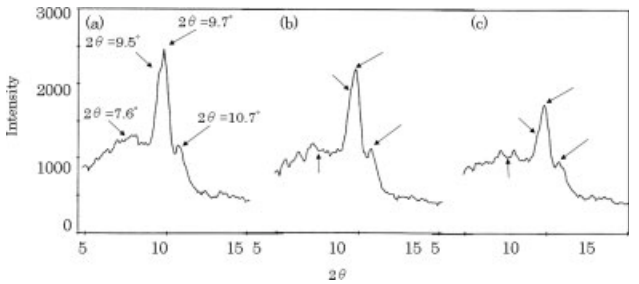

Figure 8 X-ray spectra of 70/30 PLA/PCL + 0.1 phr DCP along the equator at each layer: (a) depth of 100 μm, (b) depth of 300 μm, and (c) depth of 500 μm.

was not remarkable at 300 and 500 μm. This could be attributed to the alternation of the crystalline structure. There was no peak at 7.6° reflecting the crystalline structure of the PLA phase. Therefore, the PLA phase consisted only of an amorphous structure. The peak at 9.7°, as a representative of the peaks derived from PCL, is plotted as a function of the depth from the surface in Figure 9. The intensity was constant from the surface to a depth of 200 μm, and it decreased with increasing depth from surface. On the basis of these results, any alternations of the crystalline structure hardly occurred in the PLA matrix, but that of the PCL dispersed phase exhibited some changes; that is, the crystalline orientation was enhanced at the skin area, and the crystalline structure was changed between the skin and core area. These phenomena might be enhanced by shear flow during the injection-molding process. The dotted curve from the ultimate tensile strain of local layers (Fig. 6) has been added to Figure 9. In general, the crystalline orientation has a strong relationship with the polymer brittleness. However, the ultimate tensile strain at the initial plateau area showed a high value despite a high crystalline orientation. Thus, the behavior of the ultimate tensile strain is inconsistent

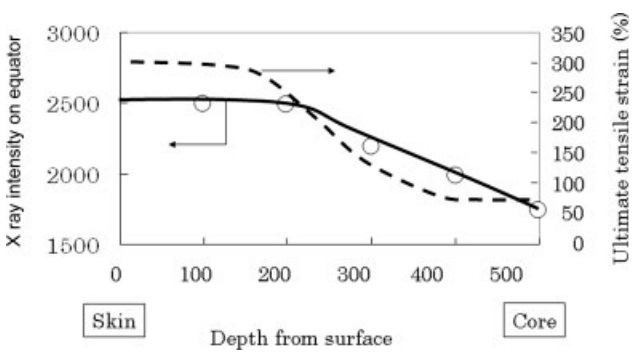

Figure 9 X-ray intensity at 9.7° and ultimate tensile strain of 70/30 PLA/PCL + 0.1 phr DCP at each layer as a function of the depth from the surface.

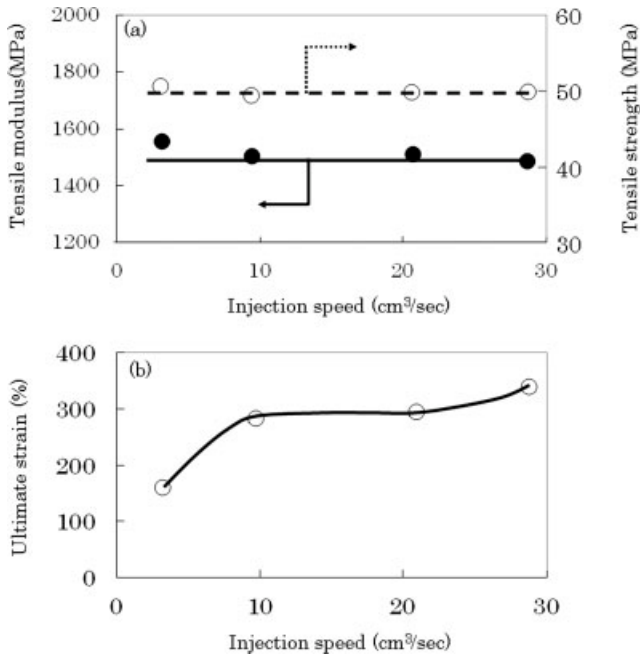

Figure 10 Tensile modulus, tensile strength, and ultimate strain of injection moldings stuffed with 70/30 PLA/PCL + 0.1 phr DCP as a function of the injection speed: (a) tensile modulus and strength and (b) ultimate tensile strain.

with the crystalline orientation. Therefore, the crystalline orientation of the PCL phase was not a primary factor of ultimate tensile strain of the blend with 0.1 phr DCP. It could be concluded that the most primary factor emphasizing ultimate tensile strain is the morphology of the PCL dispersed phase.

Effect of the injection speed on the mechanical properties of PLA/PCL blends

The effect of the injection speed on the mechanical properties of the blend containing 0.1 phr DCP was examined (Fig. 10). The tensile modulus and strength were constant throughout the whole injection speed range. However, the ultimate tensile strain increased sharply up to 9.6 cm^3/s and then remained constant from 10 to 20 cm^3/s, and a further increment could be seen beyond 20 cm^3/s. The largest ultimate tensile strain reached 340%. Thus, the high injection speed showed efficiency for improving tensile ductility. It was due to the construction of the fibrous morphology that the tensile modulus and strength were maintained but the ultimate tensile strain could be improved.

CONCLUSIONS

In this study, we verified the combinatory effects of interfacial cocrosslinking by DCP and a fibrous mor-

phology based on an *in situ* fiber reinforcing technique on the mechanical properties and the consequent production of a highly biobased, high-ductility, and biodegradable material that can be used for practical uses. According to the experimental results, the following conclusions were established. The optimum DCP concentration was 0.1 phr without splitting of the continuous dispersed phase. Further addition of DCP made the dispersed phase split, and the result of this phenomenon was that the ductility of the PCL phase could not be imparted to the PLA matrix. There was a morphology transition from the skin to core area in the injection moldings. The local layers at the skin and the intermediate parts possessing a flat and ordinary fiber morphology showed high ultimate tensile strain. This is evidence that *in situ* fiber formation is effective in the improvement of the ultimate tensile strain. The crystalline orientation of the PCL dispersed phase along the flow direction was not the main factor for the improvement of the ultimate tensile strain. The injection speed was a valuable factor to gain a high ultimate tensile strain. It was concluded that the construction of the fibrous morphology was stimulated by a high shear rate.

The authors really appreciate Seiji Watase and Kimihiro Matsukawa at the Osaka Municipal Technical Research Institute for their permission to use the X-ray diffraction machine and appropriate advice about its data analysis. They acknowledge Kouji Yamada and Kiyotaka Tomari at the Osaka Municipal Technical Research Institute for their permission to use the sliding microtome machine and useful advice concerning the mechanical properties of sliced specimens.

References

1. Shinoda, H.; Obuchi, S. Mon Eco Ind Jpn 2006, 11, 45.
2. Inao, T. J Jpn Soc Mech Eng 2006, 109, 51.
3. Inoue, K.; Serizawa, S.; Ynagisawa, T.; Iji, M. J Jpn Soc Polym Process 2006, 18, 509.
4. Kobayashi, E.; Yonezawa, J.; Takayama, S. Polym Prepr Jpn Yokohama 2005, 54, 700.
5. Katou, M.; Nishimura, H.; Kawasaki, S.; Kawaguti, T.; Yamada, M.; Sakamoto, K.; Kondou, Y. Proc Seikeikou Annu Meet 2005, 16, 193.
6. Aoki, H.; Osuga, M.; Itou, K.; Miura, T.; Shouji, N. Proc Polym Mater Forum 2005, 14, 51.
7. Okamoto, T.; Nakano, M.; Usuki, A. Polym Prepr Jpn Nigata 2005, 54, 5345.
8. Broz, M. E.; VanderHart, D. L.; Washburn, N. R. Biomaterials 2003, 24, 4181.
9. Hiljanen-Vainio, M.; Varpomaa, P.; Seppala, J.; Tormala, P. Macromol Chem Phys 1996, 197, 1503.
10. Kanamori, T.; Urayama, Y.; Kohara, H.; Shimotuma, S. Polym Prepr Jpn Kyoto 2000, 49, 4427.
11. Semba, T.; Kitagawa, K.; Ishiaku, U. S.; Hamada, H. J Appl Polym Sci 2006, 101, 1816.
12. Semba, T.; Kitagawa, K.; Ishiaku, U. S.; Hamada, H. Soc Plast Eng Annu Tech Conf, Boston, MA, 2005, 2423.
13. Semba, T.; Kitagawa, K.; Ishiaku, U. S.; Hamada, H. Soc Plast Eng Annu Tech Conf, Charlotte, NC, 2006, 2159.
14. Semba, T.; Kitagawa, K.; Ishiaku, U. S.; Kotaki, M.; Hamada, H. J Appl Polym Sci 2006, 103, 1066.
15. Semba, T.; Kitagawa, K.; Nakagawa, M.; Ishiaku, U. S.; Hamada, H. J Appl Polym Sci 2005, 98, 500.
16. Semba, T.; Kitagawa, K.; Endou, S.; Ishiaku, U. S.; Hamada, H. J Appl Polym Sci 2004, 91, 833.
17. Kitagawa, K.; Semba, T.; Hamada, H. Soc Mater Sci Jpn 1998, 47, 1270.
18. Yamada, K.; Baba, S.; Takashima, S.; Hamada, H.; Mizoguchi, M.; Kuriyama, T. Soc Plast Eng Annu Tech Conf, Chicago, IL, 2004, 718.
19. Liedauer, S.; Eder, G.; Janeschitz-Kriegl, H.; Jerschow, P.; Geymayer, W.; Ingolic, E. Int Polym Process 1993, 8, 236.
20. Kumaraswamy, G.; Issaian, A. M.; Kornfield, J. A. Macromolecules 1999, 32, 7537.